halves of the PhC–C(Ph)–C(Ph)–CPh group. We can write this as $[Cl_3Nb(\mu\text{-}O)(\mu\text{-}C_4Ph_4)NbCl_3]^{4-}$, and we then focus on the question of how to distribute electrons in the $[Nb_2(C_4Ph_4)]^{4+}$ unit.

We propose treating the C_4Ph_4 ligand as though it acquires two electrons from the metal atoms and thus becomes a coupled pair of four-electron donors, formally analogous to two Cl^- ions. We thus regard the $[Cl_3Nb(\mu\text{-}O)(C_4Ph_4)NbCl_3]^{4-}$ ion as formally analogous to a $[Cl_3Nb(\mu\text{-}O)(\mu\text{-}Cl)_2NbCl_3]^{4-}$ ion. We then have the niobium atoms in oxidation state III, and these two d^2 metal ions can form a Nb=Nb double bond. The existence of such a bond is consistent with the Nb–Nb distance of 2.61 Å. In the $Cl_2(Me_2S)Nb(\mu\text{-}SMe_2)(\mu\text{-}Cl)_2NbCl_2(SMe_2)$ molecules, where the bridging groups are larger, the Nb–Nb distance is 2.68 Å.[9]

When seen in this simplistic way, the structure and bonding in the $[Nb_4OCl_8\{(PhC)_4\}_2]^{2-}$ ion become qualitatively understandable, but it must, of course, still be recognized that the very existence of this species with its two remarkable (and apparently unprecedented) structural features is something that was not (and probably could not have been) predicted.

Acknowledgment. We thank the Robert A. Welch Foundation for support.

Supplementary Material Available: Tables of atomic positional parameters and equivalent isotropic displacement parameters for **1–3**, tables of anisotropic displacement parameters, complete tables of bond distances and angles for non-hydrogen atoms, tables of positional and isotropic thermal parameters of hydrogen atoms and the corresponding bond distances and angles, stereoviews of the unit cell contents, and a figure showing disorder modes of the THF solvent molecules (51 pages); tables of observed and calculated structure factors (102 pages). Ordering information is given on any current masthead page.

(9) Cotton, F. A.; Duraj, S. A.; Roth, W. J. *Acta Crystallogr.* **1985**, *C41*, 878.

Synthesis, Characterization, and Biological Activity of *cis*-Diammineplatinum(II) Complexes of the DNA Intercalators 9-Aminoacridine and Chloroquine

Wesley I. Sundquist, Daniel P. Bancroft, and Stephen J. Lippard*

Contribution from the Department of Chemistry, Massachusetts Institute of Technology, Cambridge, Massachusetts 02139. *Received July 14, 1989*

Abstract: The anticancer drug *cis*-diamminedichloroplatinum(II) reacts with the DNA intercalators 9-aminoacridine (9-AA) and chloroquine (CQ) to form the novel complexes *cis*-$[Pt(NH_3)_2(N9\text{-}9\text{-}AA)Cl](NO_3)$ (**1**), *cis*-$[Pt(NH_3)_2(N9\text{-}9\text{-}AA)_2](NO_3)_2$ (**2**), and *cis*-$[Pt(NH_3)_2(N1\text{-}HCQ)Cl](NO_3)_2$ (**3**). Interestingly, platinum coordinates to the deprotonated exocyclic amino group of 9-aminoacridine in **1** and **2**, with the proton being transferred to the endocyclic nitrogen atom N10, as revealed by X-ray crystal structure determinations. As a consequence, the acridine rings are asymmetrically positioned with respect to the platinum coordination plane, resulting in short (2.390 Å in **1**·MeOH and 2.458 Å in **2**·MeOH) nonbonded contacts between platinum and one of the acridine ring protons (H1). NMR spectroscopic studies demonstrated the persistence of this structure in DMF solutions of the complexes, the short Pt–H1 distances resulting in paramagnetic deshielding of the H1 protons by approximately 3.32 (**1**) and 2.25 (**2**) ppm. The Pt–H1 interactions are not agostic, however, since no reduction in the magnitude of $^1J_{Cl\text{-}H1}$ coupling is observed. In contrast to 9-aminoacridine, chloroquine preferentially coordinates to platinum via the less hindered endocyclic N1 ring nitrogen atom. Since both diastereoisomers of **3** are observed by ^1H NMR spectroscopy, rotation about the Pt–N1 bond is slow on the NMR time scale. Complexes of the general formula *cis*-$[Pt(NH_3)_2(INT)Cl]^{n+}$, where INT is a DNA intercalator such as 9-AA or CQ, have the potential to bind both covalently and intercalatively to DNA and, consequently, are potential antitumor agents. Complexes **1** and **3** were determined to be extremely toxic in animal screens, however, precluding their use as drugs.

cis-Diamminedichloroplatinum(II), *cis*-DDP, and other platinum antitumor drugs coordinate bifunctionally to DNA, inhibiting replication and transcription.[1] Biological activity in these complexes usually requires two leaving groups coordinated to platinum in cis positions.[2] Anticancer activity has also been observed in complexes of general formula *cis*-$[Pt(NH_3)_2(L)Cl]^+$, where L is an N-bound pyridine, purine, pyrimidine, or piperidine ligand.[3] This unanticipated discovery raised the possibility that the aromatic ligand L might intercalate between DNA base pairs adjacent to the site of platinum coordination, forming a pseudobifunctional adduct capable of inhibiting replication.[4] Such simultaneous intercalation and covalent coordination to DNA has been demonstrated in other classes of DNA-binding drugs such as psoralens[5] and is also a preferred mode of binding in covalent complexes formed on DNA by *cis*-DDP and ethidium bromide.[6]

The possibility that aromatic ligands might bind intercalatively upon coordination of *cis*-$[Pt(NH_3)_2(L)Cl]^+$ to DNA led us to investigate the chemistry and biological activity of analogous compounds in which L is an established intercalator. The in-

(1) Reviews: (a) Sherman, S. E.; Lippard, S. J. *Chem. Rev.* **1987**, *87*, 1153. (b) Reedijk, J. *Pure Appl. Chem.* **1987**, *59*, 181. (c) *Platinum Coordination Compounds in Cancer Chemotherapy*; Hacker, M. P., Douple, E. B., Krakoff, I. H., Eds.; Nijhoff: Boston, 1984.

(2) Reviews: (a) Hydes, P. C. *Dev. Oncol.* **1984**, *17*, 216. (b) Macquet, J.-P.; Butour, J.-L. *J. Natl. Canc. Inst.* **1983**, *70*, 899. (c) Braddock, P. D.; Connors, T. A.; Jones, M.; Khokhar, A. R.; Melzack, D. H.; Tobe, M. L. *Chem.-Biol. Interact.* **1975**, *11*, 145.

(3) Hollis, L. S.; Amundsen, A. R.; Stern, E. W. *J. Med. Chem.* **1989**, *32*, 128.

(4) Inhibition of SV 40 DNA replication in human cell extracts by coordination of *cis*-$[Pt(NH_3)_2(L)Cl]^+$ complexes has been demonstrated and will be reported elsewhere: Hollis, L. S.; Sundquist, W. I.; Burstyn, J. N.; Heiger-Bernays, W. J.; Amundsen, A. R.; Stern, E. W.; Lippard, S. J. Manuscript in preparation.

(5) Review: Cimino, G. D.; Gamper, H. B.; Isaacs, S. T.; Hearst, J. E. *Annu. Rev. Biochem.* **1985**, *54*, 1151.

(6) (a) Sundquist, W. I.; Bancroft, D. P.; Chassot, L.; Lippard, S. J. *J. Am. Chem. Soc.* **1988**, *110*, 8559. (b) Malinge, J. M.; Schwartz, A.; Leng, M. *Nucleic Acids Res.* **1987** *15*, 1779. (c) Malinge, J.-M.; Leng, M. *Proc. Natl. Acad. Sci. U.S.A.* **1986**, *83*, 6317.

0002-7863/90/1512-1590$02.50/0

tercalators 9-aminoacridine (9-AA) and chloroquine (CQ) were

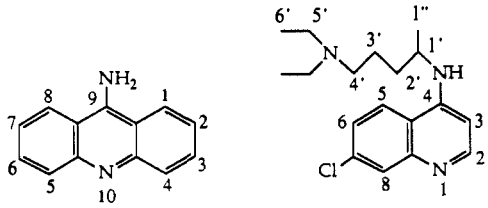

9-Aminoacridine
9-AA

Chloroquine
CQ

chosen for these studies because each has nucleophilic, endocyclic nitrogen atoms that afford potential strong binding sites for platinum. Moreover, DNA adducts formed by 9-AA and CQ have been studied extensively, and, in both cases, intercalation occurs with the endocyclic nitrogen atom residing in the major groove of DNA.[7,8] Such an intercalative geometry is stereochemically compatible with platinum coordination to DNA, which occurs preferentially at purine N7-positions in the major groove.[1]

In this paper we describe the synthesis, characterization, and biological evaluation of platinum complexes of 9-aminoacridine and chloroquine. A surprising result, of potential general importance in the field of heavy metal coordination to biological molecules, is the selective binding of platinum to the deprotonated exocyclic N9-position of 9-aminoacridine. In addition, we describe results bearing on the general question of agostic interactions in d^8 transition-metal complexes.[9]

Experimental Section

Chemicals. Reagent grade chemicals were used without further purification except where noted. Dimethylformamide (DMF) was freshly vacuum distilled from BaO and stored over molecular sieves prior to use. *cis*-DDP was prepared from K_2PtCl_4 by a modification of the method of Dhara[10] and recrystallized from aqueous 0.1 M HCl. 9-Aminoacridine free base (Sigma) was recrystallized from ethanol. Chloroquine diphosphate (Sigma) was used to prepare chloroquine free base as described below.

Removal of Chloride Ligands from *cis*-DDP. The chloride ligands of *cis*-DDP were removed with $AgNO_3$ in DMF to facilitate subsequent reactions with intercalators. To remove one chloride ligand, $AgNO_3$ (1.36 g, 8 mmol) was allowed to react with *cis*-DDP (2.40 g, 8 mmol) in 40 mL of DMF for 16 h in the dark. Silver chloride, which formed quantitatively, was removed by centrifugation. The product distribution, as determined by ^{195}Pt NMR spectroscopy, was 9% *cis*-DDP (−2092 ppm), 82% *cis*-$[Pt(NH_3)_2(O1\text{-DMF})Cl]^+$ + *cis*-$[Pt(NH_3)_2(NO_3)Cl]$ (not fully resolved, −1814 and −1800 ppm, respectively), and 9% *cis*-$[Pt(NH_3)_2(O1\text{-DMF})_2]^{2+}$ + *cis*-$[Pt(NH_3)_2(O1\text{-DMF})(NO_3)]^+$ + *cis*-$[Pt(NH_3)_2(NO_3)_2]$ (unresolved, −1593 ppm). These results are in good agreement with a previous study in which all of the resonances in the ^{195}Pt NMR spectrum were identified with the use of ^{15}N-enriched *cis*-DDP.[3] The resulting DMF solutions of monosubstituted *cis*-DDP were used without further purification.

To remove both chloride ligands from the platinum complex, $AgNO_3$ (669 mg, 3.96 mmol) was allowed to react with *cis*-DDP (600 mg, 2.0 mmol) in 40 mL of DMF for 18 h in the dark. Silver chloride was again removed by centrifugation. No products other than *cis*-$[Pt(NH_3)_2(O1\text{-DMF})_2]^{2+}$, *cis*-$[Pt(NH_3)_2(O1\text{-DMF})(NO_3)]^+$, and *cis*-$[Pt(NH_3)_2(NO_3)_2]$ were observed by ^{195}Pt NMR spectroscopy. Solutions of disubstituted *cis*-DDP were also used without further purification.

***cis*-$[Pt(NH_3)_2(N9\text{-9-AA})Cl](NO_3)$ (1).** 9-Aminoacridine free base (4.61 g, 23.7 mmol) was allowed to react with *cis*-DDP (8.0 mmol) in 40 mL of DMF following the removal of one chloride ligand from the platinum complex as described above. After 4 days the major reaction product, *cis*-$[Pt(NH_3)_2(N9\text{-9-AA})Cl](NO_3)$ (**1**), accounted for 49% of total Pt as determined by ^{195}Pt NMR spectroscopy. DMF was removed in vacuo and the resulting oil dissolved in 100 mL of methanol. The solution was centrifuged to remove insoluble material (mostly *cis*-DDP as revealed by ^{195}Pt NMR spectroscopy), and the reaction products were precipitated by slow addition into 2 L of chloroform. The resulting yellow powder was redissolved in methanol, the solution centrifuged, and the product precipitated in chloroform and collected by suction filtration. After drying, the yield of **1** was 1.76 g (42%). The solid (400 mg) was recrystallized twice from methanol by cooling a saturated solution (~10 mL) to −20 °C. Complex **1** so crystallized contains 1.0 equiv of MeOH in the lattice, as revealed by X-ray crystallography. The crystals were crushed and dried to yield 178 mg of pure *cis*-$[Pt(NH_3)_2(N9\text{-9-AA})Cl](NO_3)$ (44.5%; overall yield, 18.7%).

^{1}H NMR spectral data: δ 11.57 (d, ^3J = 8.24 Hz, 1 H), 8.16 (d, ^3J = 8.70 Hz, 1 H), 7.73 (t, av ^3J = 8.38 Hz, 1 H), 7.61 (t, av ^3J = 7.70 Hz, 1 H), 7.39 (d, av ^3J = 8.56 Hz, 2 H, unresolved), 7.34 (t, av ^3J = 7.57 Hz, 1 H), 7.23 (t, av ^3J = 7.70 Hz, 1 H). ^{13}C NMR spectral data (DMF-d_7): δ 162.8 (s, 1 C), 141.3 (s, 1 C), 138.6 (s, 1 C), 133.8 (dd, $^1J_{C-H}$ = 161.4 Hz, 1 C), 133.2 (dd, $^1J_{C-H}$ = 161.7 Hz, 1 C), 128.3 (dd, $^1J_{C-H}$ = 160.0 Hz, 1 C), 125.0 (dd, $^1J_{C-H}$ = 159.1 Hz, 1 C), 122.4 (dd, $^1J_{C-H}$ = 163.7 Hz, 1 C), 120.7 (dd, $^1J_{C-H}$ = 163.9 Hz, 1 C), 118.1 (dd, $^1J_{C-H}$ = 164.1 Hz, 1 C), 118.0 (s, 1 C), 117.3 (dd, $^1J_{C-H}$ = 163.6 Hz, 1 C), 115.7 (s, 1 C). ^{195}Pt NMR spectral data (DMF): −2206 ppm. FABMS (TEA) *m/e*: 608, $[M + TEA]^+$; 459, $[M]^+$ (matches theoretical isotope distribution); 407, $[M - Cl - NH_3]^+$; 195 $[9\text{-AA} + H^+]^+$. Anal. Calcd for $C_{13}H_{16}N_5O_3ClPt$: C, 29.98; H, 3.10; N, 13.45. Found: C, 29.79; H, 3.19; N, 13.30.

***cis*-$[Pt(NH_3)_2(N9\text{-9-AA})_2](NO_3)_2$ (2).** 9-Aminoacridine free base (1.15 g, 5.9 mmol) was allowed to react with *cis*-DDP (2.0 mmol) in 20 mL of DMF following the removal of both chloride ligands from the platinum complex as previously described. After 3 days, the major reaction product, *cis*-$[Pt(NH_3)_2(N9\text{-9-AA})_2](NO_3)_2$ (**2**), accounted for 44% of the total Pt in the ^{195}Pt NMR spectrum. Complex **2** was precipitated, dissolved in methanol, and reprecipitated in exactly the same fashion as **1**. After drying, the yield of crude **2** was 1.22 g; however, analysis by ^{195}Pt NMR spectroscopy revealed this yellow powder to be contaminated with other platinum species. The complex (150 mg) was recrystallized by slow evaporation of a 20% MeOH/$CHCl_3$ solution containing 0.2 equiv of 9-aminoacridine. Complex **2** crystallized with 1.0 equiv of $CHCl_3$ as revealed by X-ray crystallography (a = 26.419 (14) Å, b = 9.609 (6) Å, c = 27.021 (12) Å, β = 111.82 (4)°, V = 6368 (12) Å^3, $I2/a$, Z = 8). After a second recrystallization (MeOH/$CHCl_3$, no excess ligand) the crystals were crushed and dried but, nevertheless, analyzed for the presence of 0.25 equiv of $CHCl_3$, the presence of which was confirmed by ^{1}H NMR spectroscopy. The yield for this step was 32.1 mg (41.6 μmol; overall yield, 16.9%). Finally, complex **2**·MeOH was obtained by slow evaporation of a 1/1 MeOH/$CHCl_3$ solution at room temperature over the course of several days. The structure of **2**·MeOH was more precisely determined and is therefore reported herein.

^{1}H NMR spectral data: δ 10.50 (d, ^3J = 8.33 Hz, 1 H), 7.53 (t, av ^3J = 7.63 Hz, 1 H), 7.50 (d, ^3J = 8.34 Hz, 1 H), 7.43 (t, av ^3J = 7.92 Hz, 1 H), 7.32 (t, av ^3J = 7.19 Hz, 1 H), 7.22 (d, ^3J = 8.33 Hz, 1 H), 7.04 (t, av ^3J = 7.74 Hz, 1 H), 6.89 (d, ^3J = 8.34 (Hz, 1 H). ^{13}C NMR spectral data: δ 165.5 (s, 1 C), 141.2 (s, 1 C), 138.7 (s, 1 C), 134.6 (dd, $^1J_{C-H}$ = 161.1 Hz, 1 C), 133.9 (dd, $^1J_{C-H}$ = 160.5 Hz, 1 C), 127.3 (dd, $^1J_{C-H}$ = 160.9 Hz, 1 C), 124.0 (dd, $^1J_{C-H}$ = 158.1 Hz, 1, C), 123.4 (dd, $^1J_{C-H}$ = 163.8 Hz, 1 C), 121.8 (dd, $^1J_{C-H}$ = 164.5 Hz, 1 C), 118.0 (dd, $^1J_{C-H}$ = 164.2, Hz, 1 C), 117.9 (s, 1 C), 117.3 (dd, $^1J_{C-H}$ = 162.5 Hz, 1 C), 115.8 (s, 1 C). ^{195}Pt NMR spectral data (DMF): −2274 ppm. FABMS (NBA) *m/e* 832 $[M^{2+} + NO_3^- + NBA]^+$; 769, $[M^{2+} - H^+ + NBA]^+$; 752, $[M^{2+} - H^+ - NH_3 + NBA]^+$; 679, $[M^{2+} + NO_3^-]^+$; 616, $[M^{2+} - H^+]^+$ (matches theoretical isotope distribution); 599, $[M^{2+} - H^+ - NH_3]^+$; 582, $[M^{2+} - H^+ - 2(NH_3)]^+$; 405, $[M^{2+} - H^+ - 9\text{-AA}]^+$; 388 $[M^{2+} - H^+ - 2(NH_3) - 9\text{-AA}]^+$; 308, $[M^{2+}]^{2+}$; 195, $[9\text{-AA} + H^+]^+$. Anal. Calcd for $C_{26.25}H_{26.25}N_8O_6Cl_{0.75}Pt$ (**2**·0.25$CHCl_3$, dried): C, 40.87; H, 3.43; N, 14.52. Found: C, 40.88; H, 3.63; N, 14.58.

***cis*-$[Pt(NH_3)_2(N1\text{-HCQ})Cl](NO_3)_2$ (3).** Chloroquine diphosphate was converted to the free base prior to reaction with platinum. To accomplish this conversion, chloroquine diphosphate (10 g, 19.4 mmol) was dissolved in 150 mL of H_2O and diethyl ether (100 mL) was added to extract the free base. Aqueous sodium hydroxide (20 mL, 5 M, 100 mmol) was slowly added to the vigorously stirred mixture and the ether layer collected in a separatory funnel. The ether was removed in vacuo to yield 5.05 g of CQ (15.8 mmol, 82%) as a white powder.

CQ (2.43 g, 7.6 mmol) was allowed to react with *cis*-DDP (8.0 mmol) in 40 mL of DMF following the removal of one chloride ligand from the platinum complex. After 16 h, the major reaction product, *cis*-$[Pt(NH_3)_2(N1\text{-CQ})Cl](NO_3)$, accounted for 76% of the total Pt in the integrated ^{195}Pt NMR spectrum (−2299 ppm). The DMF was removed in vacuo, the resulting oil dissolved in 25 mL of ethanol, and the mixture centrifuged to remove insoluble material. The complex was precipitated by slow addition of the ethanol solution to 2 L of diethyl ether. The

(7) (a) Sakore, T. D.; Reddy, B. S.; Sobell, H. M. *J. Mol. Biol.* **1979**, *135*, 763. (b) Woodson, S. A.; Crothers, D. M. *Biochemistry* **1988**, *27*, 8904.

(8) (a) Review: Hahn, F. E. In *Mechanism of Action of Antimicrobial and Antitumor Agents; Antibiotics Vol. III*; Corcoran, J. W., Hahn, F. E., Eds.; Springer-Verlag: New York, 1975; p 58. (b) Bass, G. E.; Hudson, D. R.; Parker, J. E.; Purcell, W. P. *J. Med. Chem.* **1971**, *14*, 275.

(9) Reviews: (a) Brookhart, M.; Green, M. L. H. *J. Organomet. Chem.* **1983**, *250*, 395. (b) Brookhart, M.; Green, M. L. H.; Wong, L.-L. *Prog. Inorg. Chem.* **1988**, *36*, 1.

(10) Dhara, S. G. *Indian J. Chem.* **1970**, *8*, 193.

Table I. NMR Chemical Shift Data for 1 and 2[a,b]

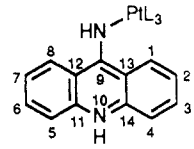

	^{1}H NMR chem shift (ppm)		^{13}C NMR chem shift (ppm)	
posn	1	2	1	2
1	11.57 (3.32)	10.50 (2.25)	128.3 (4.8)	127.3 (3.8)
8	8.16 (−0.09)	7.50 (−0.75)	125.0 (1.5)	124.0 (0.5)
2	7.34 (−0.34)	7.32 (−0.36)	120.7 (−10.9)	121.8 (−9.8)
7	7.2 (−0.45)	7.04 (−0.64)	122.4 (−9.2)	123.8 (−7.8)
3	7.73 (0.42)	7.45 (0.14)	133.8 (12.5)	134.3 (11.2)
6	7.6 (0.30)	7.5 (0.24)	133.2 (10.1)	133.9 (10.8)
4	7.39 (−0.48)	6.8 (−0.98)	117.3 (−10.5)	117.3 (−10.5)
5	7.30 (−0.48)	7.22 (−0.65)	118.0 (−9.8)	118.0 (−9.8)
9			162.8 (10.1)	165.5 (12.8)
11, 14			141.3, 138.6[c]	141.2, 138.7[c]
12, 13			118.0, 115.7[d]	117.9, 115.8[d]

[a] ^{1}H and ^{13}C NMR spectra of 9-AA, 1, and 2 were obtained in CD_3OD except for the ^{13}C NMR spectrum of 1 that was obtained in DMF-d_7 owing to the low solubility of 1 in CD_3OD. Chemical shifts are reported relative to TMS. [b] Values in parentheses show the change in chemical shift (ppm) upon platinum binding to 9-AA. Positive values denote downfield shifts versus 9-AA free base. [c] Resonances of C11 and C14 were not uniquely assigned. [d] Resonances of C12 and C13 were not uniquely assigned.

resulting white solid was redissolved in ethanol, centrifuged, and precipitated once more to remove any remaining *cis*-DDP. After drying, the yield of *cis*-$[Pt(NH_3)_2(N1\text{-CQ})Cl](NO_3)$ was 3.37 g (5.21 mmol, 69%). This complex was hygroscopic and tended to form an oil, so the chloroquine ligand was protonated at the N4′-position (designated HCQ) to give a more crystalline solid. Protonation was accomplished by addition of HNO_3 (1.08 mmol, 0.54 mL of 2.0 M stock, 1.4 equiv) to a saturated solution of *cis*-$[Pt(NH_3)_2(N1\text{-CQ})Cl](NO_3)$ (500 mg, 773 μmol, ~150 mM) in ethanol. The product, *cis*-$[Pt(NH_3)_2(N1\text{-HCQ})Cl](NO_3)_2$ (3), was recrystallized twice from ethanol (−80 °C). The yield for the protonation step was 301 mg (424 μmol, 55%; overall yield, 38%).

^{1}H NMR spectroscopic data (chemical shifts from both diastereoisomers of 3 are reported if resolved: δ 9.51 (d, ^4J = 1.90 Hz, 1 H), 8.58, 8.56 (d, av ^3J = 6.46 Hz, 1 H), 8.26, 8.23 (d, av ^3J = 8.52 Hz, 1 H), 7.50, 7.47 (dd, av ^3J = 9.44 Hz, ^4J = 2.39 Hz, 1 H), 6.62, 6.60 (d, av ^3J = 6.46 Hz, 1 H), 3.89 (m, 1 H), 2.59 (m, 4 H), 2.56 (m, 2 H), 1.67 (m, 2 H), 1.61 (m, 2 H), 1.33 (d, av ^3J = 6.35 Hz, 3 H), 1.03 (m, 6 H). ^{195}Pt NMR spectral data (3, CH_3OH): −2288 ppm. FABMS (*cis*-$[Pt(NH_3)_2(N1\text{-CQ})Cl]NO_3$, NBA) *m/e*: 584, $[M^+]^+$ (matches theoretical isotope distribution); 567, $[M^+ - NH_3]^+$; 550 $[M^+ - 2(NH_3)]^+$; 549, $[M^+ - Cl]^+$; 512, $[M^+ - NEt_2]^+$. Anal. Calcd for $C_{18}H_{33}N_7O_6Cl_2Pt$: C, 30.47; H, 4.69; N, 13.82. Found: C, 30.44; H, 4.76; N, 13.72.

Instrumentation and Analytical Methods. One- and two-dimensional correlated (COSY) ^{1}H NMR spectra were obtained on a Varian VXR500 NMR spectrometer (500 MHz). One-dimensional NOE experiments were performed on a Varian XL300 NMR spectrometer (300 MHz) by subtracting selectively irradiated from off-resonance irradiated spectra. All chemical shifts (δ) were referenced to internal tetramethylsilane. ^{13}C NMR spectra were obtained on a Bruker WM270 spectrometer (67.93 MHz). ^{1}H–^{13}C heteronuclear-correlated (HETCOR) NMR spectra were obtained on Varian XL300 and VXR500 NMR spectrometers. ^{13}C NMR chemical shifts were referenced relative to the solvent peak and are reported versus TMS. ^{1}H and ^{13}C NMR spectra were obtained in CD_3OD, except where noted. ^{195}Pt NMR spectra were measured on a Varian VXR500 NMR spectrometer (107.25 MHz), with chemical shifts referenced relative to an external standard of 0.1 M K_2PtCl_4 in 0.1 M DCl/D_2O (−1624 ppm). Chemical shifts are reported relative to H_2PtCl_6 in D_2O (0 ppm).

Positive ion, fast atom bombardment mass spectra were obtained in matrices of 3-nitrobenzyl alcohol (NBA) or triethanolamine (TEA). Elemental analyses were performed by Atlantic Microlabs Inc. Platinum complexes were tested for antitumor activity by using a murine S180a screen as previously described.[3]

NMR Assignments. The ^{1}H NMR spectrum of 9-aminoacridine has been assigned previously.[11] The ^{13}C NMR spectrum of 9-aminoacridine was assigned on the basis of a HETCOR spectrum (for protonated carbon atoms) and diagnostic chemical shifts (for quarternary carbon atoms).[12] The ^{1}H and ^{13}C NMR spectra for 1 and 2 were assigned as follows (for numbering scheme, see Table I): the proton resonance at very low field was assigned as H1 on the basis of the crystal structures of 1·MeOH and 2·MeOH that reveal the unique location of this proton above the platinum square plane. Protons H2, H3, and H4 could then be assigned from the connectivity observed in a COSY spectrum. The ^{13}C NMR resonances of carbon atoms C1–C4 were subsequently assigned from a HETCOR spectrum, and the ^{13}C NMR resonances of C5–C8 were assigned on the basis of their chemical shifts, which correspond pairwise to the analogous carbons C1–C4 (Table I). ^{13}C NMR resonances of the quarternary acridine carbons were assigned on the basis of their chemical shifts,[12] but the C11 and C14 and C12 and C13 pairs could not be uniquely differentiated. The remaining proton resonances (H5–H8) were assigned from carbon atom connectivity observed in the HETCOR spectrum. The ^{1}H NMR spectra of CQ and *cis*-$[Pt(NH_3)_2(N1\text{-HCQ})Cl](NO_3)_2$ were readily assigned on the basis of chemical shifts, scalar coupling, and the connectivity observed the COSY spectra.

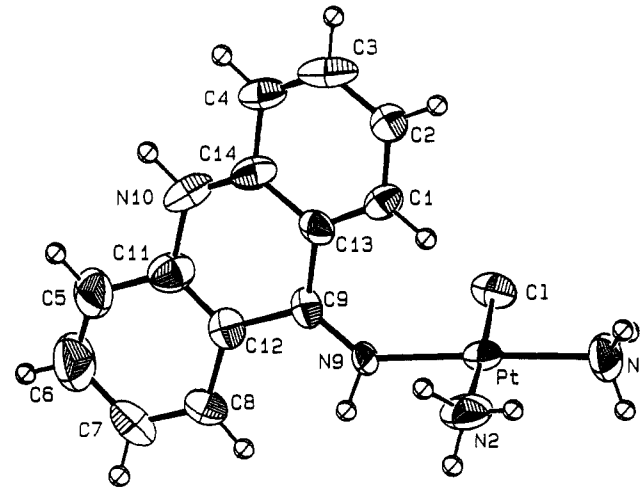

Figure 1. Structure of *cis*-$[Pt(NH_3)_2(N9\text{-9-AA})Cl]^+$ cation showing the 40% probability thermal ellipsoids and atom-labeling scheme.

X-ray Crystallography. A crystal of 1-MeOH was sealed in glass capillary next to a pool of mother liquor to prevent solvent loss. 2-MeOH was mounted on a glass fiber with epoxy cement. Crystal quality was checked by open counter ω-scans on several strong, low-angle reflections. Unit cell parameters were obtained from a least-squares fit of 25 centered reflections with $2\theta > 11.3°$. Three standard reflections were measured periodically throughout the data collection. A decay correction was applied to the data from 1-MeOH that showed a 8.3% loss of intensity over the course of the data collection. Data were reduced and the structures solved by using the programs in the X-ray crystallographic package TEXSAN.[13] Corrections were applied for Lorentz and polarization effects and for absorption (1·MeOH, ψ scans and DIFABS;[14] 2·MeOH, analytical correction).

Positions of the platinum atoms were determined from Patterson maps, and all remaining non-hydrogen atoms were revealed in subsequent difference Fourier maps. Non-hydrogen atoms were refined anisotropically while hydrogen atoms were placed at calculated positions (C–H = 1.10 Å) and constrained to "ride" on atoms to which they were attached. Scattering factors for neutral atoms and corrections for anomalous dispersion were taken from ref 15. Further details of data collection, reduction, and refinement of the structures of 1-MeOH and 2-MeOH are summarized in Table S1 (supplementary material).

1·MeOH. A bright yellow, blocklike crystal of 1·MeOH of dimensions 0.5 mm × 0.2 mm × 0.2 mm was selected, and preliminary study on a diffractometer revealed a triclinic space group, either $P1$ (No. 1) or $P\bar{1}$ (No. 2).[16] Statistical analysis favored the centrosymmetric space group,

(11) Acheson, R. M. In *Acridines, 2nd Ed., Heterocyclic Compounds*; Acheson, R. M., Ed.; Wiley and Sons: New York, 1973; Vol. 9, pp 696–698.

(12) Levy, G. C.; Lichter, R. L.; Nelson, G. L. *Carbon-13 Nuclear Magnetic Resonance*; 2nd ed.; Wiley and Sons: New York, 1980.

(13) *TEXSAN (1987), TEXRAY structure analysis system*, Version 4.0: Molecular Structure Corp.: College Station, TX, 1987.

(14) Walker, N.; Stuart, D. *Acta Crystallogr., Sect. A: Found. Crystallogr.* **1983**, *A39*, 158.

(15) *International Tables for X-ray Crystallography*; Ibers, J. A., Hamilton, W. C., Eds.; Kynoch: Birmingham, England, 1974; Vol. IV, pp 99, 149.

(16) *International Tables for X-Ray Crystallography*; Hahn, T. Eds.; Reidel: Dordrecht, The Netherlands, 1983; Vol. A, pp 102–105, 185–188.

Table II. Mean Values of Selected Bond Lengths and Angles in **1**·MeOH and **2**·MeOH[a,b]

	1·MeOH	2·MeOH		1·MeOH	2·MeOH		1·MeOH	2·MeOH
				Bond Lengths (Å)				
Pt–Cl	2.31 (1)		C6–C7	1.50 (4)	1.46 (2)	C1–C2	1.36 (6)	1.36 (2)
Pt–N2	2.06 (2)		C8–C12	1.42 (2)	1.37 (2)	C2–C3	1.40 (3)	1.42 (2)
N9–C9	1.32 (2)	1.28 (1)	C9–C13	1.46 (7)	1.44 (1)	C4–C14	1.40 (5)	1.47 (2)
N10–C14	1.35 (6)	1.34 (1)	C13–C14	1.41 (3)	1.41 (2)	C5–C11	1.46 (3)	1.46 (2)
C1–C13	1.46 (3)	1.44 (2)	Pt–N1	2.04 (3)	2.04 (1)	C7–C8	1.38 (4)	1.37 (2)
C3–C4	1.36 (3)	1.33 (4)	Pt–N9	1.99 (2)	2.013 (8)	C9–C12	1.46 (6)	1.47 (1)
C5–C6	1.32 (9)	1.26 (2)	N10–C11	1.36 (6)	1.34 (1)	C11–C12	1.36 (3)	1.41 (2)
				Bond Angles (deg)				
Cl–Pt–N1	88.6 (8)		N10–C11–C12	121 (3)	123 (1)	C1–C2–C3	123 (3)	121 (1)
Cl–Pt–N9	91.1 (5)		C8–C12–C9	122 (2)	122 (1)	C3–C4–C14	120 (2)	120 (1)
N1–Pt–N9 (cis)		90.0 (4)	C9–C12–C11	120 (2)	119 (1)	C5–C6–C7	118 (2)	123 (1)
N2–Pt–N9 (cis)	88 (2)		C1–C13–C14	118 (2)	117 (1)	C7–C8–C12	124 (2)	122 (1)
Pt–N9–C9	136 (1)	129.1 (7)	N10–C14–C4	118 (2)	119 (1)	N9–C9–C13	122 (4)	122 (1)
C2–C1–C13	118 (2)	122 (1)	Cl–Pt–N2	179 (2)		N10–C11C5	118 (2)	120 (1)
C2–C3–C4	120 (2)	120 (1)	N1–Pt–N2	93 (3)		C5–C11–C12	121 (2)	118 (1)
C6–C5–C11	122 (2)	120 (1)	N1–Pt–N9 (trans)	178 (2)	177.9 (4)	C8–C12–C11	117 (3)	119 (1)
C6–C7–C8	118 (2)	117 (1)	C4–C14–C13	121 (3)	120 (1)	C1–C13–C9	122 (2)	122 (1)
N9–C9–C12	122 (2)	123 (1)	C11–N10–C14	122 (2)	120 (1)	C9–C13–C14	120 (2)	121 (1)
C12–C9–C13	116 (2)	115 (1)				N10–C14–C13	120 (2)	121 (1)

[a] Atoms are numbered as in Figures 1 and 2. Bond lengths and angles were averaged where duplicated. [b] Numbers in parentheses represent errors in the last digit assigned as the larger of either the individual error or the rms deviation from the mean.

Scheme I

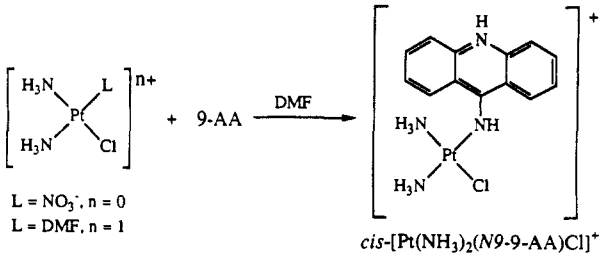

L = NO_3^-, n = 0
L = DMF, n = 1

cis-$[Pt(NH_3)_2(N9\text{-}9\text{-}AA)Cl]^+$

Scheme II

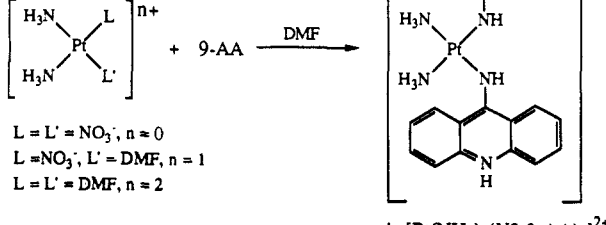

L = L' = NO_3^-, n = 0
L = NO_3^-, L' = DMF, n = 1
L = L' = DMF, n = 2

cis-$[Pt(NH_3)_2(N9\text{-}9\text{-}AA)_2]^{2+}$

and this choice was confirmed by successful refinement of the structure. Crystal data for $C_{14}H_{20}N_5O_4ClPt$ are as follows: a = 17.524 (7) Å, b = 17.625 (7) Å, c = 7.198 (5) Å, α = 100.61 (5)°, β = 96.61 (6)°, γ = 68.98 (5)°, V = 2037 (4) Å^3, Z = 4, fw = 552.76, ρ_{calcd} = 1.802 g cm^{-3}. For 4547 unique, observed [$I > 3\sigma(I)$] reflections, and 451 variable parameters, the discrepancy indices were R_1 = 0.058 and R_2 = 0.085. Each asymmetric unit contains two nearly identical *cis*-$[Pt(NH_3)_2(N9\text{-}9\text{-}AA)Cl]^+$ cations of the same chirality (designated A and B). The structure and atom-labeling scheme of the A cation are shown in Figure 1, and a listing of selected interatomic distances and angles is given in Table II. Fractional coordinates, anisotropic thermal parameters, and a listing of observed and calculated structure factors for **1**·MeOH are given in Tables S2–S4, respectively (supplementary material).

2·$CHCl_3$. An orange, platelike crystal of **2**·MeOH (0.20 mm × 0.15 mm × 0.075 mm) was selected for study. The crystal belonged to the orthorhombic system with the space group *Fddd* (No. 70) uniquely determined from systematic absences in the data.[16] Crystal data for $C_{27}H_{30}N_8O_7Pt$ are as follows: a = 9.6785 (8) Å, b = 12.544 (4) Å, c = 44.009 (9) Å, V = 12 584 (5) Å^3, Z = 16, fw = 773.68, ρ_{calcd} = 1.633 g cm^{-3}. For 1611 unique, observed [$I > 3\sigma(I)$] reflections, and 201 variable parameters, the discrepancy indices were R_1 = 0.042 and R_2 = 0.055. The structure and atom-labeling scheme of *cis*-$[Pt(NH_3)_2(N9\text{-}9\text{-}AA)_2]^{2+}$ are shown in Figure 2, and a listing of selected interatomic distances and angles is given in Table II. Fractional coordinates, anisotropic thermal parameters, and a listing of observed and calculated structure factors for **2**·MeOH are given in Tables S5–S7, respectively (supplementary material).

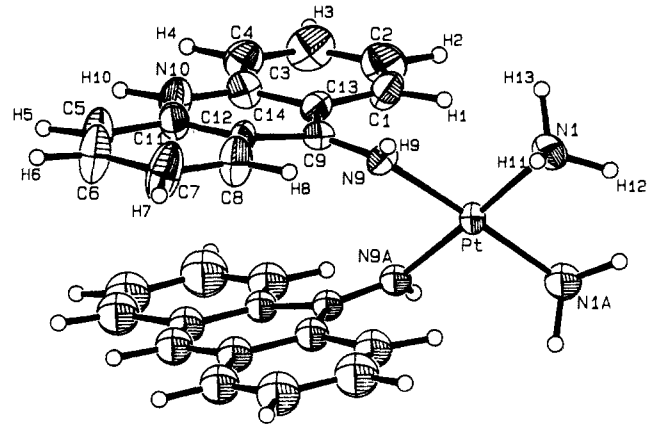

Figure 2. Structure of *cis*-$[Pt(NH_3)_2(N9\text{-}9\text{-}AA)_2]^{2+}$ cation showing the 30% probability thermal ellipsoids and atom-labeling scheme.

Results

Syntheses and Structures of *cis*-$[Pt(NH_3)_2(N9\text{-}9\text{-}AA)Cl](NO_3)$ (1) and *cis*-$[Pt(NH_3)_2(N9\text{-}9\text{-}AA)_2](NO_3)_2$ (2). Removal of one or both chloride ligands from *cis*-DDP with silver nitrate in DMF facilitates subsequent ligand substitution reactions and allows control of the stoichiometry of substitution.[3,17] This strategy was therefore used to prepare platinum complexes in which either one (Scheme I) or both (Scheme II) chloride ligands of *cis*-DDP were replaced by 9-aminoacridine. These reactions were conveniently monitored with ^{195}Pt NMR spectroscopy, the chemical shifts of the products being used to assign ligands in the coordination spheres of **1** and **2** (−2206 and −2274 ppm, respectively).[3,18]

Complexes **1**·MeOH and **2**·MeOH were isolated as single crystals suitable for X-ray diffraction studies following purification procedures described in the Experimental Section. ORTEP diagrams showing the platinum coordination spheres of **1** and **2** are presented in Figures 1 and 2, respectively. Selected interatomic distances

(17) Lippert, B.; Pfab, R.; Neugebauer, D. *Inorg. Chim. Acta* **1979**, *37* (1), L495.

(18) (a) Review: Pregosin, P. S. *Coord. Chem. Rev.* **1982**, *33*, 512. (b) Appleton, T. G.; Hall, J. R.; Ralph, S. F. *Inorg. Chem.* **1985**, *24*, 4685.

and angles are given in Table II. In both structures, platinum coordinates to the deprotonated N9 amino position of 9-aminoacridine. Since the geometry of **2**·MeOH was more precisely determined, only it will be discussed in detail, except where significant differences occur in the structures.

The platinum coordination geometry in both **1**·MeOH and **2**·MeOH is nearly square-planar; in the latter compound, the metal sits on a C_2 symmetry axis. All ligand angles are within 4° of idealized values (Table II), and no significant deviations from planarity are observed (average deviation in **2**·MeOH, 0.04 Å). The Pt–Cl and Pt–NH_3 bond lengths are normal, with no appreciable lengthening of Pt–NH_3 bonds trans to 9-aminoacridine. A single proton was found for each of the sp^2-hybridized N9 and N10 amino groups in difference Fourier maps of **2**·MeOH, establishing that 9-aminoacridine occurs as the imino tautomer. Removal of an N9 amino proton shortens the Pt–N9 and N9–C9 bonds and increases the Pt–N9–C9 angles as compared to a platinum-coordinated, fully protonated exocyclic amino group.[6a] Protonation of the N10 position increases the C11–N10–C14 angles slightly, and all such angles in both structures fall within the range (125 ± 3°) for a protonated endocyclic sp^2 nitrogen atom in a six-membered ring (deprotonated N, 116 ± 3°).[19]

Angles within the 9-aminoacridine rings of **1**·MeOH and **2**·MeOH are normal (120 ± 6°), and the rings are planar (average deviation in **2**·MeOH, 0.04 Å), although the N9 atoms are drawn significantly out of the planes (deviation in **2**·MeOH, 0.25 Å). The π system in the acridine rings is delocalized, showing the expected shortening of C1–C2, C3–C4, C5–C6, C7–C8 (average C–C bond in **2**·MeOH, 1.33 Å; bond order, $^5/_3$) compared to the remaining C–C bonds (average C–C in **2**·MeOH, 1.44 Å; bond order, $^4/_3$). The same pattern of long and short bonds is observed in the crystal structure of N10-protonated 9-aminoacridine itself (average short C–C bond, 1.36 Å; average long C–C bond, 1.41 Å).[20]

The trigonal geometry about N9 tips the acridine ring over the platinum square plane in **1**·MeOH (Figure 1). Similarly, the two acridine rings lie over opposite sides of the platinum square plane in the structure of **2**·MeOH and are related by a crystallographic 2-fold rotation axis (Figure 2). The asymmetric coordination of 9-aminoacridine in these complexes renders the acridine ring protons inequivalent and brings the H1 atoms close to the platinum atom. The average Pt–Cl distance in **1**·MeOH is 3.22 (1) Å, and the Pt–H1 distance, calculated by generating H1 in an idealized geometry 1.10 Å from Cl, is 2.390 Å. In the structure of **2**·MeOH, the analogous average distances are 3.17 (1) Å (Pt–Cl) and 2.458 Å (Pt–H1). The acridine ring of **1**·MeOH is nearly perpendicular to the Pt square plane (average dihedral angle, 105.0°; average torsion angles, Pt–N9–C9–C12 = 165 (1)° and Pt–N9–C9–C13 = 12 (3)°). The acridine rings of **2**·MeOH, however, are significantly tilted with respect to the coordination plane (dihedral angle, 114.94°; torsion angles, Pt–N9–C9–C12 = 143.1 (1)° and Pt–N9–C9–C13 = −36 (1)°), allowing intramolecular stacking of the two acridine rings in this complex, the interplanar ring distance being ~3.5 Å. Both complexes show extensive intermolecular stacking of acridine rings as well as numerous hydrogen-bonding interactions between the platinum ligands, counterions, and lattice solvent molecules. In particular, imino protons on the acridine N10 positions are stabilized by hydrogen-bonding interactions with the lattice methanol molecules in **1**·MeOH and the nitrate anions in **2**·MeOH.

As shown by NMR spectroscopic studies, acridine rings of **1** and **2** also exist in the imino tautomeric form in solution. Protons on H9 and H10 of **1** were observed directly in DMF-d_7 solution at 9.10 and 11.8 ppm, respectively. Selective irradiation of the H9 resonance resulted in a strong nuclear Overhauser enhancement of the H8 (18.5%), but not the H1 (<3%), resonance. This result indicates that the asymmetric coordination of 9-aminoacridine revealed in the crystal structure of **1**·MeOH (average H9···H8 = 1.74 Å; average H9···H1 = 3.74 Å) also persists in solution. Selective irradiation of the H10 resonance resulted in a strong NOE (12.7%) of both the H4 and H5 resonances, as expected (average H10···H4 = 2.31 Å, average H10···H5 = 2.33 Å).

Scheme III

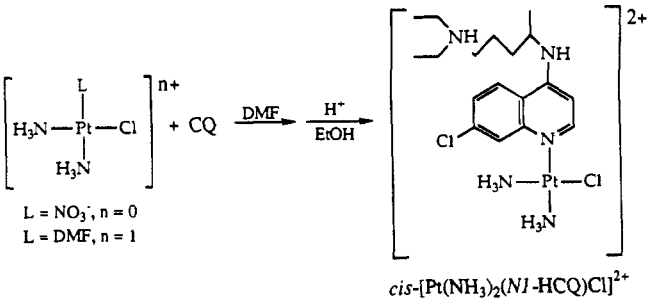

The positive charge on the protonated acridine rings of **1** and **2** may be delocalized onto the C1-, C3-, C6-, C8-, C9-, C11-, and C14-positions, much as in the 9-aminoacridinium cation itself. This delocalization is reflected in the ^{13}C NMR spectra of **1** and **2**, expecially at the C3-, C6-, and C9-positions, for which shifts to lower field by 10–11 ppm occur upon platinum binding and proton transfer (Table I). Similar ^{13}C NMR chemical shifts are observed at these positions upon protonation of 9-aminoacridine.[11] Delocalization of the positive charge is also reflected in the ^1H NMR spectra of **1** and **2**; protons H1 and H3 are shifted downfield compared with their positions in the NMR spectrum of 9-aminoacridine free base (Table I).

The most striking feature in the ^1H NMR spectra of **1** and **2** is the extremely low field shift of the H1 resonances (Table I), resulting from close contacts with the platinum atoms. These protons are shifted downfield by 3.32 ppm (**1**) and 2.25 ppm (**2**) versus 9-aminoacridine free base. The $^1J_{C1-H1}$ coupling constants in **1** and **2** reveal the extent to which the C1–H1 bonds in these complexes experience agostic interactions with the platinum centers.[9] No reduction was observed in $^1J_{C1-H1}$ values, compared to the analogous $^1J_{C8-H8}$ coupling constants (**1**, $^1J_{C1-H1}$ = 160.0 Hz, $^1J_{C8-H8}$ = 159.1 Hz; **2**, $^1J_{C1-H1}$ = 160.9 Hz, $^1J_{C8-H8}$ = 158.1 Hz). The $^1J_{C1-H1}$ coupling constants in **1** and **2** are also essentially unchanged from those of 9-aminoacridine itself (9-AA, $^1J_{C1-H1}$ = 158.2 Hz; 9-AA·HCl, $^1J_{C1-H1}$ = 163.4 Hz). Therefore, no evidence exists for agostic bonding in these compounds. The nature of the Pt···H1 interactions is considered more fully in the Discussion.

Synthesis and Characterization of *cis*-[Pt$(NH_3)_2$(*N*1-HCQ)Cl]$(NO_3)_2$. Chloroquine free base (CQ) reacted with *cis*-DDP following removal of one chloride ligand from platinum to give *cis*-[Pt$(NH_3)_2$(*N*1-CQ)Cl]$^+$ as the major reaction product. The reaction, monitored by ^{195}Pt NMR spectroscopy, yielded primarily the N1-bound product, which accounted for 76% of the platinum in the final integrated spectrum (−2299 ppm, methanol solution). No resonance attributable to an N4-bound isomer was observed. The complex, isolated as described in the Experimental Section, was protonated at the N4′ position with dilute nitric acid and purified by recrystallization from ethanol to yield *cis*-[Pt$(NH_3)_2$(*N*1-HCQ)Cl]$(NO_3)_2$ (**3**) (Scheme III).

Platinum coordination at the N1-position of chloroquine was established by mass spectrometric and NMR spectroscopic studies. In the ^1H NMR spectrum of **3**, protons adjacent to the platinated N1 position shifted downfield by 1.73 ppm (H8) and 0.25 ppm (H2) compared to their positions in chloroquine free base (Table III). In contrast, all other chloroquine protons shift by less than 0.2 ppm upon platinum coordination (data not shown), although protons H4′ and H5′ shift downfield upon subsequent protonation of N4′ (Table III).

Resonances arising from both diastereoisomers of *cis*-[Pt$(NH_3)_2$(*N*1-HCQ)Cl]$^{2+}$ were observed in the ^1H NMR spectrum of **3** (Table III), although chemical shift differences were small and not fully resolved for most protons. The maximum chemical shift separation occurred for the H3 proton, positioned midway

(19) Singh, C. *Acta Crystallogr.* **1965**, *19*, 861.
(20) Talacki, R.; Carrell, H. L.; Glusker, J. P. *Acta Crystallogr.* **1974**, *B30*, 1044.

Table III. ^{1}H NMR Chemical Shift Data for **3**[a,b]

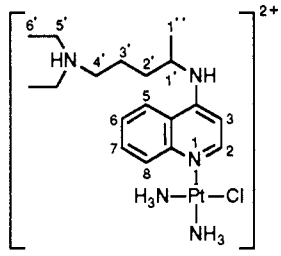

posn	^{1}H NMR chem shift (ppm)[c]	posn	^{1}H NMR chem shift (ppm)[c]
H2	8.59, 8.58 (0.25, 0.24)	H2′	1.75 (0.04)
H3	6.64, 6.61 (0.13, 0.10)	H3′	1.71 (0.12)
H5	8.27, 8.25 (0.07, 0.05)	H4′	2.88 (0.45)
H6	7.49, 7.48 (0.12, 0.11)	H5′	2.93 (0.44)
H8	9.51 (1.73)	H6′	1.16 (0.18)
H1′	3.94 (0.17)	H1″	1.34 (0.02)

[a] Spectra were obtained in CD_3OD. Chemical shifts are reported relative to TMS. [b] Values in parentheses show the change in chemical shift (ppm) upon platination (N1) and protonation (N4′) of chloroquine free base. Positive values denote downfield shifts versus CQ free base. [c] Chemical shifts for both diastereomers are given where resonances were resolved.

between the two asymmetric centers in the cation. Observation of both diastereomers indicates that rotation about the Pt–N1 bond is slow on the NMR time scale, since fast rotation would average out the effective chirality of the platinum center.

Biological Studies of *cis*-[Pt(NH$_3$)$_2$(*N*9-9-AA)Cl](NO$_3$) (1) and *cis*-[Pt(NH$_3$)$_2$(*N*1-HCQ)Cl](NO$_3$)$_2$ (3). The antitumor activities of **1** and **3** were investigated in a murine sarcoma 180 ascites (S180a) screen.[3] Complete experimental toxicity and antineoplastic data are given in Table S8 (supplementary material). Surprisingly, the complexes are both far more toxic than either *cis*-DDP or the free intercalators alone and are therefore not reasonable candidates for further evaluation as antitumor drugs. Complex **1** was toxic at 5 mg/kg of mouse, the lowest concentration tested. Complex **3** was also toxic at 5 mg/kg of mouse and showed no significant antitumor activity at lower doses.[21] Any antineoplastic activity in these complexes is therefore obscured by their toxicity, although the cause of this toxicity has not been determined.

Discussion

9-Aminoacridine Complexes. Aminoacridines comprise an especially well characterized class of DNA intercalative drugs. 9-Aminoacridine was selected from this class as an attractive candidate for platinum binding studies for several reasons. Being the most basic of the simple aminoacridines, 9-aminoacridine was expected to have the high degree of nucleophilicity required for coordination to the cationic platinum center.[22a] In addition, the presence of three fused aromatic rings was anticipated to lead to a stable intercalative interaction with DNA following covalent binding of platinum. In view of the preference for platinum complexes to coordinate at purine N7-positions, it was anticipated that the complex *cis*-[Pt(NH$_3$)$_2$(*N*10-9-AA)Cl]$^+$, if it could be synthesized, might bind bifunctionally to DNA via intercalation of the acridine ring and simultaneous covalent attachment of platinum in the major groove. Another reason for choosing 9-aminoacridine was its symmetry and relative simplicity compared to other intercalators. These factors diminish the number of possible platinum coordination sites and stereoisomers encountered in preliminary studies with 3,6-diaminoacridine (proflavin). Finally, 9-aminoacridine was considered an attractive target ligand because the intercalative binding of this molecule to nucleic acids is relatively well understood. A crystal structure of 9-aminoacridine with $(CpG)_2$ reveals that 9-aminoacridine probably intercalates with the endocyclic N10-position in the major groove and the exocyclic N9 amino group in the minor groove.[7] This stereochemistry is compatible with the preference for platinum to bind major groove residues in DNA, such as purine N7 positions.

Although the amino tautomer of 9-aminoacridine predominates in organic solvents,[22b] both nitrogen atoms can react with electrophiles. For example, 9-aminoacridine is preferentially acetylated with acetic anhydride at the N9-position,[23] while smaller alkyl halides such as methyl or ethyl iodide alkylate at the N10-position.[24] We initially expected platinum coordination at the endocyclic N10-position, owing to its greater basicity. As described above, however, platinum coordinates preferentially to the exocyclic N9-position of 9-aminoacridine. No products attributable to platinum binding at the N10-position were detected by ^{195}Pt NMR spectroscopy, and we estimate the regiospecificity of Pt for N9 to be at least 20/1 over the N10-position. Presumably, coordination at N9 is sterically favored, especially in the five-coordinate transition state. Platinum coordination at the exocyclic amino group is accompanied by proton transfer to N10; complex **1** exists as the imino tautomer in both solution and solid states. The increased acidity of Pt(II)-coordinated amine ligands is well-known.[25] It is uncertain, however, whether 9-aminoacridine tautomerization precedes or follows platination of N9, since platinum(II) can react directly with aryl amines,[26] but should react even more rapidly with any minor ligand imino tautomers present in solution.

A consequence of sp^2 hybridization of the N9 imino group is the asymmetric orientation of 9-aminoacridine ligands of **1** and **2** with respect to the platinum coordination plane. In both complexes, the H1 proton is held within 2.5 Å of the platinum center (Figures 1 and 2). Similar Pd(II)···H–C and Pt(II)···H–C interactions (M···H < 3.0 Å) have been described as "agostic", a term that implies formation of a two-electron, three-center bond resulting from formal sharing of the electron pair in the C–H bond with an empty metal orbital.[9] The C–H bond order is thereby reduced, decreasing the $^1J_{C-H}$ coupling in a manner diagnostic of agostic bonding in static systems. In complexes **1** and **2**, however, the $^1J_{C1-H1}$ coupling constants are not diminished relative to $^1J_{C8-H8}$ nor are the values significantly different from those of 9-aminoacridine itself. We therefore conclude that the Pt···H1–C1 interactions in **1** and **2** are predominantly 'anagostic' and arise simply as a result of the asymmetric coordination of the 9-aminoacridine ligand.

Although short Pd(II)···H and Pt(II)···H contacts in other complexes have been described as agostic,[9b] they too may arise simply from rigid or sterically constrained ligands that result in short nonbonded metal–proton contacts. The bonding in such complexes has been investigated to varying degrees, but both experimental[27] and theoretical[28] considerations suggest that C–H interactions with d^8 metals are weak and may even be electronically

(21) Six female CFW mice were implanted with 2 × 10^6 S180 tumor cells intraperatoneally (ip) on day 0. Mice were subsequently treated on day 1 with an ip injection of an aqueous solution of **1** (0.5 mL, 5 mg/kg of mouse), resulting in an average decreased life span of 77% versus untreated controls. Similar treatment with **3** at a dose of 5 mg/kg resulted in an average decreased life span of 62%.

(22) Adcock, B. In *Acridines, 2nd ed., Heterocyclic Compounds*; Acheson, R. M., Ed.; Wiley and Sons: New York, 1973: Vol. 9, (a) p 110; (b) p 121.

(23) (a) Albert, A.; Goldacre, J. *J. Chem. Soc.* **1943**, 454. (b) Wilkenson, J. H.; Finar, I. L. *J. Chem. Soc.* **1946**, 115.

(24) Albert, A.; Ritchie, B. *J. Chem. Soc.* **1943**, 158.

(25) Lippert, B.; Arpalahti, J.; Krizanovic, O.; Micklitz, W.; Schwarz, F.; Trötscher, G. In *Platinum and Other Metal Coordination Compounds in Cancer Chemotherapy*; Nicolini, M., Ed.; Nijhoff: Boston, 1988; p 563.

(26) (a) Weil, T. A.; Schmidt, P. J.; Orchin, M. *Inorg. Chem.* **1969**, *8*, 2138. (b) Davies, G. R., Hewertson, D. W.; Mais, R. H. B.; Owston, P. G.; Patel, C. G. *J. Chem. Soc. A* **1970**, 1873. (c) Pizzotti, M.; Cenini, S.; La Monica, G. *Inorg. Chim. Acta* **1978**, *33*, 161. (d) Haghighi, S.; McAuliffe, C. A.; Hill, W. E.; Kohl, H. H.; Friedman, M. E. *Inorg. Chim. Acta* **1980**, *43*, 113. (e) Auf der Heyde, T. P. E.; Foulds, G. A.; Thornton, D. A.; Watkins, G. M. *Spectrosc. Lett.* **1981**, *14*, 455. (f) Kong, P.-C.; Rochon, F. D. *Inorg. Chim. Acta* **1982**, *61*, 269. (g) Albinati, A.; Moriyama, H.; Rüegger, H.; Pregosin, P. S.; Togni, A. *Inorg. Chem.* **1985**, *24*, 4430. (h) Cross, R. J.; Davidson, M. F.; Rocamora, M. *J. Chem. Soc., Dalton Trans.* **1988**, 1147.

(27) (a) Albinati, A.; Anklin, C. G.; Pregosin, P. S. *Inorg. Chim. Acta* **1984**, *90*, L37. (b) Anklin, C. G.; Pregosin, P. S. *Mag. Res. Chem.* **1985**, *23*, 671.

(28) Saillard, J.-Y.; Hoffmann, R. *J. Am. Chem. Soc.* **1984**, *106*, 2006.

unfavorable. The large Pt-N9-C9 angle of 136° in complex **1**·MeOH, for example, actually *increases* the Pt···H1 distance compared with the value that would result if the angle were 120°, suggesting a repulsive interaction between these atoms. Similarly, the acridine rings in complex **2**·MeOH tilt by 24.9° with respect to the Pt coordination plane, a movement that also increases the Pt···H1 distance. Our results therefore support the conclusion that remote (>3 bond) Pd(II)···H and Pt(II)···H interactions observed in many crystal structures result from steric interactions that position protons in the empty space above the metal plane rather than from any attractive, agostic interactions.[28]

Deshielding of nuclei that lie above the coordination plane in square-planar d^8 complexes results from the paramagnetic anisotropy of the metal ion.[29] Complexes **1** and **2** provide excellent examples of this effect since crystal structures reveal that the H1 atoms are positioned above the Pt coordination plane, and NMR spectroscopic studies demonstrate that these nuclei are deshielded relative to the analogous H8 protons (Table I). The magnitude of paramagnetic deshielding should decrease with increasing Pt···H1 distance and as the proton moves away from the z axis.[29b,30] This effect offers a qualitative explanation for the greater deshielding of the H1 proton in **1** versus **2** since the Pt···H1 distance is significantly shorter in the former (**1**·MeOH, Pt···H1 = 2.390 Å; **2**·MeOH, Pt···H1 = 2.458 Å), and the H1 proton of **1** is also slightly closer to the idealized z axis, subtending angles of 15° and 19.6° in **1**·MeOH and **2**·MeOH, respectively.

One eventual goal of these studies is the use of platinum–intercalator complexes to deliver a reactive platinum moiety to the major groove of DNA following intercalation. It is possible that *cis*-$[Pt(NH_3)_2(N9\text{-}9AA)Cl](NO_3)$ would not serve this function since the N9 amino group normally resides in the minor groove of a 9-AA–DNA complex[7] (althouth this preference may not be absolute[31]). We reasoned that a different intercalator, less hindered at the endocyclic nitrogen atom and sterically more crowded at the exocyclic amino group, should favor platinum binding at the endocyclic position, yielding a complex with platinum bound on the side of the intercalator facing the major groove. Chloroquine, a DNA intercalator believed to bind in the same orientation as 9-aminoacridine,[8] meets these criteria. The quinoline ring nitrogen atom (N1) of chloroquine is less hindered than the corresponding ring nitrogen (N10) of 9-aminoacridine, and the alkyl chain sterically inhibits the exocyclic amino group (N4) from binding platinum.

As anticipated, platinum coordinates preferentially at the endocyclic N1-position to form *cis*-$[Pt(NH_3)_2(N1\text{-}HCQ)Cl](NO_3)_2$. The site of platinum coordination in **3** was determined by monitoring the downfield shift of protons (H2 and H8) on the chloroquine ring. As expected, the H8 proton is deshielded to a greater extent than H2, since it is held closer and more directly above the platinum atom. Similar downfield shifts have been observed for platinum binding to N1 in other substituted quinolines.[27]

Observation of both diastereomers of *cis*-$[Pt(NH_3)_2(N1\text{-}HCQ)Cl]^{2+}$ demonstrates that rotation about the Pt–N1 bond in this complex is slow on the ^1H NMR spectroscopic time scale. To our knowledge, rotation about Pt(II)–quinoline bonds has not been studied, but the rate of rotation about Pt–N7 purine bonds in platinum–6-oxopurine complexes has been examined by ^1H NMR spectroscopy.[32] In such complexes, rotation is slow only when the other platinum ammine ligands are replaced by more hindered alkylamines. Rotation about Pt–N1 in *cis*-$[Pt(NH_3)_2(N1\text{-}HCQ)Cl]^{2+}$ is therefore slower than about Pt–N7 in the *cis*-$\{Pt(NH_3)_2\}^{2+}$ purine complexes, apparently because of greater steric hindrance of the 6-membered ring in quinoline versus the 5-membered ring in 6-oxopurine.

A long-term objective of this work is the design and synthesis of multifunctional molecules that bind DNA in predictable ways and that may have novel drug activities. The antitumor activity of *cis*-$[Pt(NH_3)_2(L)Cl]^+$ (where L is an N-bound pyridine, purine, pyrimidine, or piperidine ligand) complexes suggests that molecules having the potential to bind DNA both intercalatively and covalently might exhibit enhanced antitumor activity as compared to compounds binding in one mode or the other. Both *cis*-$[Pt(NH_3)_2(N9\text{-}9\text{-}AA)Cl]NO_3$ and *cis*-$[Pt(NH_3)_2(N1\text{-}CQ)Cl](NO_3)$ have been tested for antitumor activity in a murine S180a screen, but the extreme toxicity of both complexes obviates any chemotherapeutic potential. Nevertheless, the successful preparation of these and other platinum–intercalator complexes[6c,33] demonstrates that it is possible to design and synthesize platinum complexes with novel DNA-binding capabilities. Further chemical modifications, guided in part by studies[4] that reveal the structural and functional consequences that occur when these compounds bind DNA, could well lead to the desired biological activities.

Acknowledgment. This work was supported by U.S. Public Health Service Grant CA 34992 (to S.J.L.) from the National Cancer Institute and NIH National Research Service Award GM 11880-01 from the National Institute of General Medical Sciences (to D.P.B.). W.I.S. is grateful to the Whitaker Health Sciences Fund for a predoctoral fellowship. Antitumor animal testing was performed at Engelhard Corp. under the direction of Dr. L. S. Hollis. We also thank Dr. Hollis for helpful discussions and Engelhard Corp. for a loan of K_2PtCl_4, from which platinum complexes were synthesized. FAB mass spectra were obtained with the assistance of Dr. C. Costello at the facility supported by NIH Grant RR 00317 (Principal Investigator, Prof. K. Biemann) from the Biotechnology Resources Branch, Division of Research Resources.

Supplementary Material Available: Tables containing X-ray crystallographic data for compounds **1**·MeOH and **2**·MeOH (Table S1), positional parameters (Tables S2 and S5), thermal parameters (Tables S3 and S6), and the biological activity in a Murine tumor screen (Table S8) (13 pages); structure factors for compounds **1**·MeOH and **2**·MeOH (Tables S4 and S7) (68 pages). Ordering information is given on any current masthead page.

(29) (a) Buckingham, A. D.; Stephens, J. P. *J. Chem. Soc.* **1964**, 4583. (b) Miller, R. G.; Stauffer, R. D.; Fahey, D. R.; Parnell, D. R. *J. Am. Chem. Soc.* **1970**, *92*, 1511.

(30) Pople, J. A.; Schneider, W. G.; Bernstein, H. J. *High Resolution Nuclear Magnetic Resonance*; McGraw-Hill Inc.: New York, 1959; p 178.

(31) (a) Nuss, M. E.; Marsh, F. J.; Kollman, P. A. *J. Am. Chem. Soc.* **1979**, *101*, 825. (b) Young, P. R.; Kallenbach, N. R. *J. Mol. Biol.* **1981**, *145*, 785.

(32) (a) Cramer, R. E.; Dahlstrom, P. L. *J. Am. Chem. Soc.* **1979**, *101*, 3679. (b) Marcelis, A. T. M.; Van der Veer, J. L.; Zwetsloot, C. M.; Reedijk, J. *Inorg. Chim. Acta* **1983**, *78*, 195.

(33) (a) Review: Lippard, S. J. *Acc. Chem. Res.* **1978**, *11*, 211. (b) Bowler, B. E.; Ahmed, K. J.; Sundquist, W. I.; Hollis, L. S.; Whang, E. E.; Lippard, S. J. *J. Am. Chem. Soc.* **1989**, *111*, 1299.